THE GALACTIC WARP IN HIPPARCOS

R.L. Smart, R. Drimmel, M.G. Lattanzi
Osservatorio Astronomico di Torino, Pino Torinese, TO 10025, Italy

ABSTRACT

We examine the positions and proper motions of a sample of OB Hipparcos stars for evidence of the warp in our galaxy. This examination is carried out by a comparison of the observations with a sophisticated simulation of the galaxy discussed in Drimmel et al. (1997). The spatial distribution of these early type stars in the galaxy confirms a warped structure. The kinematic signature is, however, not consistent with a long lived warp as defined by the spatial distribution.

Key words: space astrometry; galactic kinematics; warpage; early-type stars.

1. INTRODUCTION

The warp of our galaxy was first seen in HI observations (Kerr 1957) as starting just outside the solar circle and reaching a height of 3 kpc above and below the plane at 16 kpc from the galactic center in the north and south hemispheres respectively. It then turns back towards the galactic plane in the south. A number of driving mechanisms have been suggested for this warp e.g. a misaligned large dark halo (Binney 1978), tidal interactions with a companion galaxy (Hunter & Toomre 1969), intergalactic magnetic fields (Battaner et al. 1990) and intergalactic winds (Kahn & Woltjer 1959). However, still no theoretical consensus exists, partially because of the lack of observational constraints. If the results of the Hipparcos satellite can constrain the kinematics of the warp then it may help eliminate some of the present possibilities.

In this paper we first discuss the sample and determination of photometric distances, then we discuss the spatial and kinematical evidence for a warp separately.

2. HIPPARCOS SAMPLE

In Smart & Lattanzi (1996) we showed that if the Galactic warp were described by a rigid tilted disc model then the maximum proper motion signature would be of the order of 10 mas/yr, easily measurable by the Hipparcos satellite. As a result we successfully submitted an ADHOC proposal to obtain the proper motions of all OB stars with a measured parallax < 2 mas (to exclude local features) between galactic longitudes 70 and 270. These were chosen as stars that would best show the warp effect, as they presumably follow the HI gas plane, and could be seen out to large distances. The parallaxes were not requested as the relative error of photometric parallaxes is expected to be less than that of trigonometric parallaxes for these stars due to their distance; distances based on the HIC spectral typing and HIP photometry were calculated.

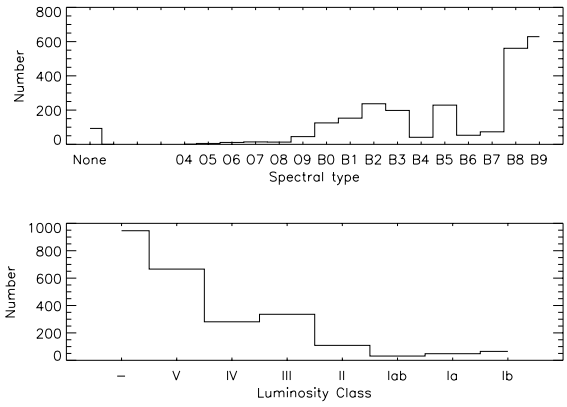

Figure 1. Spectral type and luminosity class distributions from the Hipparcos input catalogue. Note there is a large number of stars without any luminosity classification.

The resulting sample consists of 2482 stars, of which 60 had no spectral classification at all, and 947 had no luminosity class. Figure 1 shows the distribution of spectral types and luminosity classes taken directly from the input catalogue. Figure 2 shows the log of the number distribution for given apparent magnitude bins. The straight line is a best fit to the 5.5...7.0 magnitude bins. If the stars were uniformally distributed this line would have a slope of 0.6; we find a slope of 0.52. From this fit we estimate the completeness of the sample to be about 90 per cent up to $V = 8$ mag.

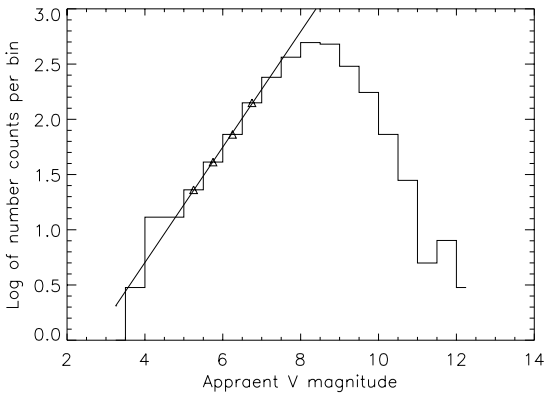

Figure 2. The log of the number density per apparent magnitude bin. The deviation from the straight line, fitted to the magnitude range 5.5...7.0, illustrates the sample completeness.

3. PHOTOMETRIC DISTANCES

For the sample that had full spectral classification the determination of distance was straight forward, adopting Schmidt-Kaler (1982) as our primary source for absolute magnitude and color calibrations. For the 947 stars without luminosity classification five methods were used to determine the absolute magnitude directly. We note that from a standpoint of luminosity classes these stars are almost degenerate in color, i.e. for a given luminosity class the color changes less than 0.3 from O5–B9.5.

1. For stars with published H_β magnitudes the absolute magnitude was calculated using the calibration in Schmidt-Kaler (1982). There were 125 stars with H_β of which did not have full HIC spectral classification. Figure 3 shows a plot of the two calibrations tested, Reed (1995) for H_β less than 2.69 and Schmidt-Kaler (1982), along with the magnitudes and H_β measurements of the fully classified stars. There appears to be a slightly shallower gradient to the HIC versus H_β fit that maybe real or maybe due to small number statistics in the large H_β end. This can be more fully examined when the full Hipparcos Catalogue is released.

2. For stars with U magnitudes, found from the Geneva Photometric Database (Mermiliod et al. 1997), we found the $Q_{UBV} = (U-B) - 0.72(B-V)$, then the intrinsic $(U-B)_o = 0.015 + 1.235 Q_{UBV}$ (Reed 1993) and finally the absorption as given by $A_V = 3.1 * [(U-B) - (U-B)_o]/0.72$. (We also tested a more complex calibration for $(U-B)_o$ versus Q_{UBV} from Cameron-Reed 1995, but found the one above worked better.) We thus have an 'observational absorption' estimate. We now assume that the published spectral type found is approximately correct, and using this absorption find what the distance of the star would have to be for the 7 luminosity classes (Ia...V). These distances are then fed to a model of galactic absorption (Spergel et al. 1997) to give us 7 estimates of the absorption; the one closest to the observed absorption is taken to correspond to the correct luminosity class. There are 288 stars with U magnitudes which do not have full HIC spectral classification.

3. Again, for stars with U magnitudes we have observational absorption, so combined with observed V and I colors we can calculate $(V-I)_o = (V-I) - .516 A_V$. As Figure 4 shows, Q_{UBV} is correlated with the $(V-I)_o$, and gives an indication if the star is either a giant (Ia,Iab,Ib,II) or a subgiant/dwarf (III,IV,V), as only one of the corresponding $(V-I)_o$ will be close to that of the given spectral class. This same process was tried using Q_{BVI}, but there is not a similar correlation.

4. Finally, for all stars (i.e. the sample of 947 without HIC classification) we can estimate a luminosity classification based on $B-V$ and colors. The method is similar to that using Q_{UBV} and absorption, only differing in that the initial $(B-V)_o$ comes from the calibration of the spectral type and the 7 tested luminosity classes, and the 'observational absorption' comes from $A_V = 3.1 * [(B-V) - (B-V)_o]$.

5. As method four but using published I magnitudes and $A_V = .48 * [(V-I) - (V-I)_o]$ for 947 stars.

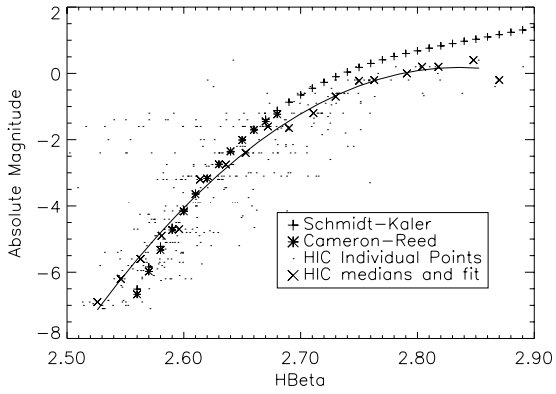

Figure 3. The correlation between H_β and M_V as given by two calibrations and as found from the stars in this sample with full HIC spectral classification.

For all methods the stars with full spectral classification in the HIC were not changed, but were used as a control group on the capability of a particular method. There is probably some correlation for certain stars as sometimes a spectroscopist may have used one of these methods to refine their own classification. Also, in each of these comparisons of the photometrically derived absolute magnitudes and the spectroscopically derived ones, the overall error includes error in the classification, cosmic error, error in the absolute magnitude calibration, error in the observed magnitudes and finally error in the photometrically derived absolute magnitude. We estimate

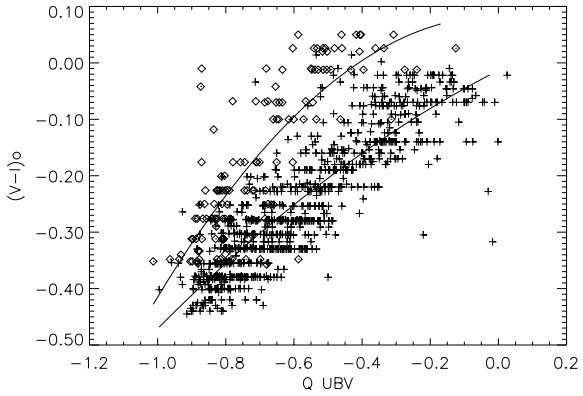

Figure 4. The correlation between Q_{UBV} and $(V-I)_o$, the two lines are fits to giant stars (Ia,Iab,Ib,II) and subgiants/dwarf stars (III,IV,V).

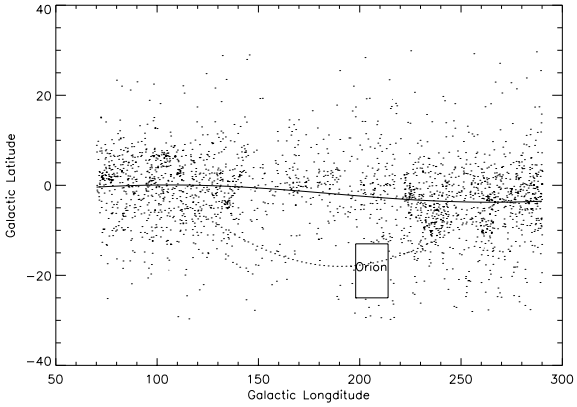

Figure 5. The variation of galactic longitude with latitude. Stars within the Orion box were excluded from the fits of the sine curve. The orientation of Gould's belt is shown as the dashed curve.

the error introduced by all but the last source (i.e. the photometric method adopted) to be of the order of 1.0 magnitude following reasoning described in Smart et al. 1996b. From a comparison of the derived absolute magnitude and that using the HIC full spectral classifications we find the error in the photometrically produced absolute magnitudes to be of the order of 0.75 magnitudes for methods one and four, 1.7 magnitudes for methods two and three and 2.5 for method five. We note that the error for method four is an underestimate as it is a method with a higher correlation with the HIC spectral type, but we also note that it only uses the most precise observational quantities (B and V from Hipparcos) so we would expect it to be slightly better than the other approaches. The final absolute magnitudes came from a weighted average of the results of the five methods only when the HIC spectral classification was not complete – when complete we accepted that.

4. SPATIAL WARP

Neglecting the precession of the warp, we assume the warp structure follows the general form:

$$Z_w = h(r)\sin(\phi - \phi_w) \qquad (1)$$

where Z_w is the systematic warp height, $h(r)$ a height function, ϕ the galactocentric azimuth, and ϕ_w the phase angle of the warp. Based roughly on the HI map of the warp as presented in Burton (1988), the simple height function $h(r) = a(r - r_w)^2$ has been adopted, r_w being the radius where the warp starts and a a height parameter. This is meant to only describe the amplitude variation of the warp at galactocentric radii in the vicinity of the solar circle. Radio observations also indicate that the sun is close to the line of nodes; we therefore adopted $\phi_w = 0$ for all synthetic catalogues utilized here.

The above formulation of the warp was incorporated into the galaxy model and different diagnostics were examined for evidence of the warp. For the following only a nearly complete sample (834 stars to $m_V = 8.$) of our data was used, as the incomplete portion may be strongly biased in its spatial distribution. The first test is a simple plot of l versus b; because of our perspective a warp will be seen as a sinusoidal curve in the data. Figure 5 shows a plot of the data where a sine pattern can be seen. For these plots stars in the Orion region were removed.

However, from an analysis of synthetic catalogues, both with and without warps, we find that the sinusoidal variation seen in the data may be due to local structure rather than the large scale warp structure. Though the amplitude of the sine curve as seen in the data is significantly greater than that of nowarp simulations, and is within the error of the warp simulations, the phase of the fitted sine curve is not well determined. This indicates that while the sinusoidal signature is consistent with a warp, it is not a sensitive diagnostic for the warp parameters.

One example of such local structure is Gould's Belt. It's orientation is overplotted in Figure 5 as a dotted line. With our $\pi < 2$ mas selection criteria we have effectively eliminated this feature which dominates the OB star distribution within 0.5 kpc. This filtering of the feature can be confirmed by inspecting a X versus Z plot ([X,Y,Z] being heliocentric cartesian coordinates with X,Y parallel to the galactic plane and the Y axis pointed in the direction of rotation) which shows no sign of this structure for our sample.

A better diagnostic plot is a Z versus Y plot. As the stars in our dataset are close to the line of nodes (by association with the sun) an Y,Z plot will be nearly linear at any given distance from the galactic center. The slope in a Z versus Y is a signature of the warp independent of the sun's height above the plane. We expect this slope to increase with galactocentric distance, due to the increasing warp amplitude. In Table 1 we list the slopes and standard deviations in different distance bins using 10 simulations without and with a warp ($r_w = 7.0$ kpc and $a = 0.05$), all other galactic parameters being kept constant. In the last column are the slopes measured for the data, which indicate the existence of a warp starting inside

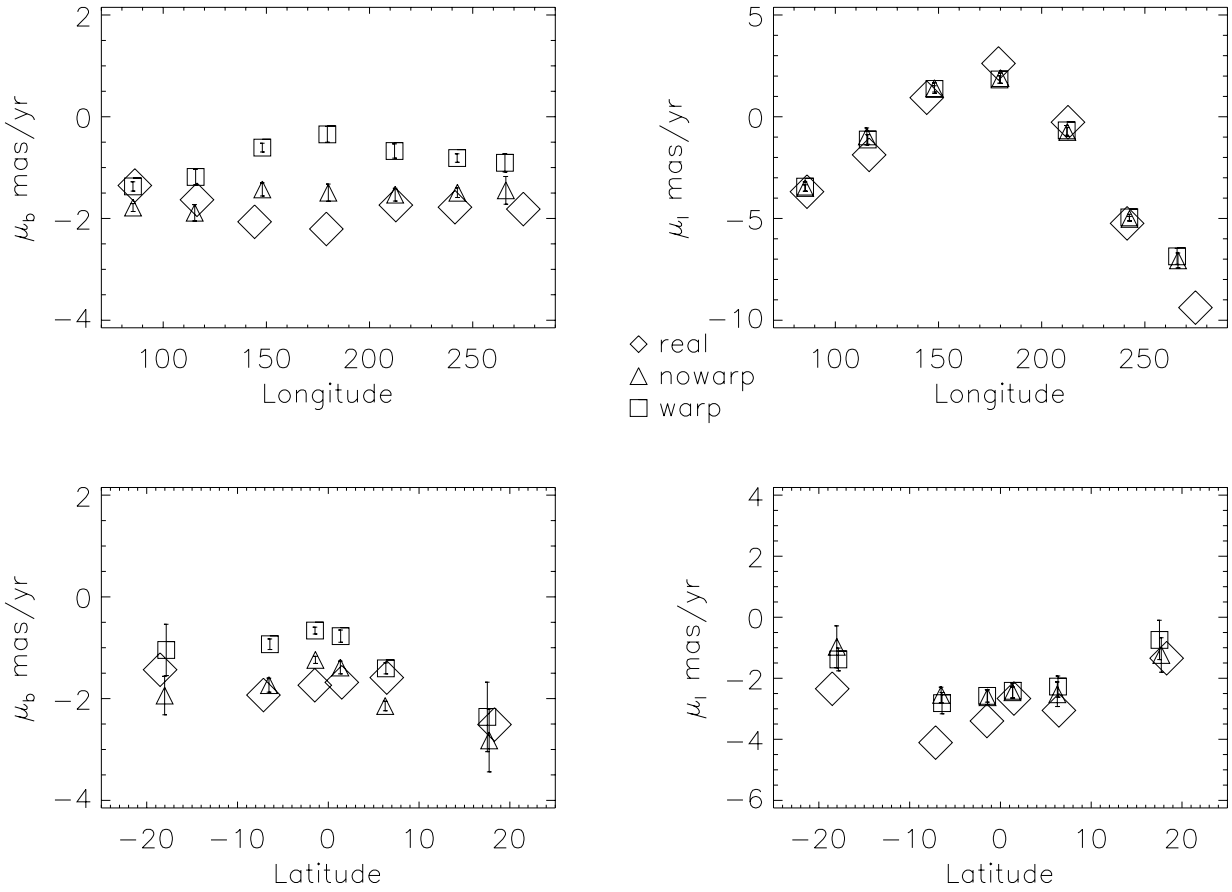

Figure 6. The variation of proper motions with position. The error bars represent the standard deviation of that point from 10 simulations. The larger symbols are the data.

Table 1. Z versus Y slopes, simulations and data.

Component	No warp	Warp	Data
All Distances	.000 ± .008	.032 ± .009	.035
r <8.5	.000 ± .006	.025 ± .007	.030
8.5< r <9.5	.002 ± .024	.046 ± .013	.043

the solar circle with an amplitude consistent with the HI data.

Finally, the only other factor that will affect the apparent distribution of the stars is absorption. As shown in Smart et al. (1996a), absorption will tend to hide the warp rather than accentuate it so removal of absorption effects will increase the warp signature.

5. KINEMATIC WARP

To evaluate the kinematic effect of a warp we employ a model for the systematic velocities consistent with the spatial warp described above. Stars revolving about the galactic center must have a systematic vertical velocity

$$V_w = \omega_*(r)h(r)\cos(\phi) \qquad (2)$$

if they are to maintain a spatial warp over a long period of time. Here $\omega_*(r)$ is the average angular velocity of the stars. We have neglected the precession of the warp, this is expected to be below the accuracy of Hipparcos (Smart & Lattanzi 1996).

We have several diagnostic plots for examination of the kinematic warp. In Figure 6 we show the variation of galactic proper motions with respect to galactic coordinate for two simulations (no warp: $a = 0$ and warp: $a = 0.05$, $r_w = 7.0$ kpc) along with the data. As discussed in Smart & Lattanzi (1996), if the warp is approximated by a tilted disk outside a given radius, then the signature in a l versus μ_b plot should be of the order of 10 mas. In Figure 7 we repeat the graph of that signature with a correction to the sign of the proper motions derived in that work. From a comparison of Figure 6 and 7 we conclude that the previous model used is kinematically unrealistic.

As expected, the variation of μ_l with both l and b is independent of the warp, and therefore these two

plots allow us to set both the slope of the rotation curve and two components of the solar velocity ($V_\odot$ and $U_\odot$). The mean offset of the μ_b plots allow us to set the third component of the solar velocity, and the variation with l will indicate if the warp is evident in the proper motions: the no warp case shows very little variation of μ_b with l while the warp case shows a 'concave' variation with l. The data however shows no variation, or may even be 'convex', that is better fitted by the no warp case.

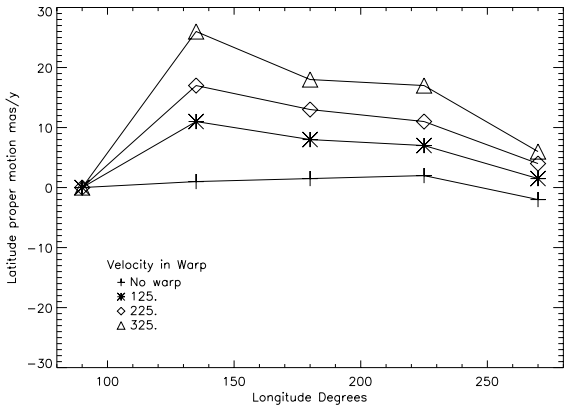

Figure 7. Corrected Figure 2 from Smart & Lattanzi 1996 showing correlation of latitude proper motion with longitude for a tilted disk model. If this model was correct we expect to see the signature indicated by a 'velocity in the warp' of 225 km/s, i.e. the diamonds.

A quantitative test of the kinematical signature is to compare the observed systematic vertical velocities with the systematic velocity as predicted for a long lived warp (Equation 2). If we ignore asymmetric drift then:

$$V_w = \frac{V_c}{r} h(r) cos(\phi) \qquad (3)$$

where V_c is the circular velocity at the radius of the star. In the height function $h(r)$ the warp parameters $r_w = 7.0$ kpc and $a = 0.05$; were found to be reasonable from the spatial warp work. We can compare this to the observed vertical velocity corrected for the motion of the sun, i.e.:

$$v_z = \frac{4.74 d \mu_b}{\cos b} + W_\odot - (V_\odot \cos l + U_\odot \sin l) \tan b. \quad (4)$$

In general these two velocities are not equal due to the peculiar velocities, and for a given star the relation will be $v_z = V_w + W_* - S_* \tan b$, S_* being a component of the peculiar motion parallel to the galactic plane. We can assume that W_* will average to zero for an appropriately large volume, and that $(S_* \tan b)$ will average to a small value, resulting in a strong correlation between the predicted velocities, V_w, and the observed velocities, v_z. In Figure 8 we plot the results for a comparison of these two velocities for simulations of no warp, the warp predicted from the spatial data ($r_w = 7.0$ kpc and $a = 0.05$) and a warp with twice the amplitude ($r_w = 7.0$ kpc and $a = 0.1$). Plotted are the bounds for the mean slope ± two sigma of the slope from 40 runs. As can be seen at the 90 per cent level (two sigma) the various simulations do not overlap. The data, however, does not give a line that falls in any of the three sets of simulations, therefore the kinematic signature is again significantly different from that expected from a long lived warp.

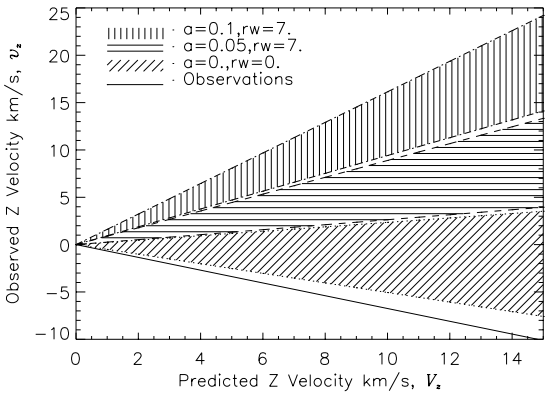

Figure 8. Correlation of observed Z velocity, Equation 4, for the observations (the solid line) versus that predicted by using Equation 3 directly. The hashed areas are two sigma boundaries for forty simulations using the parameters indicated in the legend.

A more direct test for a kinematic signature of the warp is in a plot of $v_z/cos\phi$ versus r. If the velocities have any relation to the warp we would expect a positive correlation. The problem with the interpretation of this data is that we are dominated by errors. Ignoring errors in the solar motion the errors in $\cos^{-1}\phi, r$ and $v_z/\cos\phi$ are:

$$\sigma_{c_p^{-1}} = (\sigma_d . c_b \sqrt{\frac{r^2 c_l^2}{(R_o - d.c_b.c_l)^4} + \frac{(d.c_b - R_o c_l)^2}{((R_o - d.c_b.c_l) r)^2}}$$

$$\sigma_{v_z/c_p} = \frac{4.74}{c_b c_p} \sqrt{\sigma_{\mu_b}^2 d + \sigma_d^2 \mu_b^2 + \sigma_{c_p^{-1}}^2 d^2 \mu_b^2 c_p^2}$$

$$\sigma_r = \frac{d.c_b - R_o c_l}{r} \sigma_d c_b$$

$$c_p = \cos\phi; \quad c_b = \cos b; \quad c_l = \cos l$$

(d in kpc if μ_b is in mas). Therefore, considering typical values for a star at the limit of our sample ($\phi = 0.$, $d = 3$ kpc, $\mu_b = 1$ mas/yr, $\sigma_{\mu_b} = 1$ mas/yr, σ_d=0.2d, l=180), $\sigma_{v_z/\cos\phi}$=17km/s, but the effect of the warp at this distance from Equation 3 is only 15km/s. The v_z error alone is greater than the effect and the error in R adds to this difficulty.

We therefore invested a large amount of effort in removing outliers and deciding which fitting method to use to search for a correlation. As the example above shows, cutting using relative errors would actually remove stars that reflect the warp velocity, therefore following the work of Torra et al. (this volume) we assume that those stars with absolute circular or vertical velocities 46km/s greater than the mean velocity at the given radius were probable runaways that could safely be removed. Then we also removed all

stars which had a velocity in either coordinate greater than three standard deviations of the overall velocities.

We derived the correlation with both a robust minimization of the mean absolute deviation, and with a normal least squares including errors on both coordinates. Correlations were compared using the sample with full HIC spectral classification and also with the whole sample (i.e. including photometrically derived classifications). Figure 9 shows that this correlation is marginally negative, for the data and this is consistently the case using all combinations of different fitting routines, outlier rejection and sample selection described above. Also plotted are the hashed two sigma regions from 40 simulations of the no warp, warp and large warp models as defined above. We see that the fit to the observations (the lowest solid line) is only marginally consistent with the nowarp envelope, and is definitely inconsistent with the warp simulations.

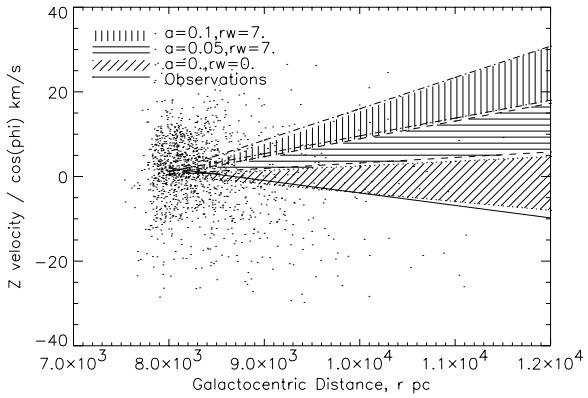

Figure 9. The variation of velocity with galactocentric radius. The points are the observations, the hashed areas are two sigma boundaries for forty simulations using the parameters indicated in the legend, and the lowest solid line is the fit to the observations.

CONCLUSIONS

We have confirmed the spatial warp of the galaxy. We do not see the kinematic signature that corresponds to a long lived warp. Comparison with simulated catalogues indicates this non-detection is significant. Therefore we conclude that the warp as seen in young OB stars is not a long lived structure as would be produced by a misaligned halo. Such a short lived warp could be produced by an encounter with a companion galaxy, for example the recently discovered companion dwarf galaxy in Sagittarius (Ibata et al. 1994).

ACKNOWLEDGMENTS

We acknowledge discussions with Drs Binney, Blaauw, and Casertano during the preparation of this paper. We would also like to thank Dr J.C. Mermilliod for providing the photometric data from the Geneva Observatory database. RLS acknowledges the support of a Royal Society fellowship. RLS and RD acknowledge the support of Torino University.

REFERENCES

Battaner, E., Florido, E., Sanchez-Saavedra, M. L., 1990, A&A, 236, 1

Binney, J., 1978, Mon. Not. R. Astron. Soc. 183, 779

Burton, W. B., 1988, in Galactic and extragalactic radio astronomy, SAAS Fee 21, pp 295–358, ed. W. B. Burton, B. Elmgreen, & R. Genzel, Berlin and New York, Springer-Verlag.

Drimmel, R., et al., 1997, ESA SP–402, this volume

Hunter, C., Toomre, A., 1969, Astron. J. 155, 747

Ibata, R. A., Gilmore, G., Irwin, M. J., 1994, Nature 370, 194

Kahn, F., Woltjer, L., 1959, Astron. J. 130, 705

Kerr, F., 1957, Astron. J. 62, 93

Mermiliod, J.-C., Mermilliod, M., Hauck, B., 1997, A&ASS, In press.

Reed, B. C., 1993, PASP, 105, 1465

Reed, B. C., 1995, PASP, 107, 907

Schmidt-Kaler, T., 1982, Landolt/Bornstein, Numerical Data and Functional Relationship in Science and Technology, ed. K. Schaifer & H. H. Voigt

Smart, R. L., Drimmel, R., Lattanzi, M. G., 1996a, New Horizons from Multi-Wavelength Sky Surveys, IAU Sym 179, Kulwer Academic Press, ed. B. M. Clean, In press.

Smart, R. L., Lattanzi, M. G., 1996, A&A, 314, 104

Smart, R. L., Lattanzi, M. G., Drimmel, R., 1996b, Widefield Spectroscopy, ed. E. Kontizas & M. Kontizas, In press

Spergel, D., Malhoptra, S., Blitz, L., 1997, Spiral Galaxies in the Near-IR, ESO-Garching, ed. D. Minnitti & H. Rix, In press